An Adaptive Neuro-Fuzzy Inference System with the Comparative Metaheuristic Aware Renewable Energy-Based Multifunction Onboard Charger-Based Ev

Benedict Josly G*[1], Prakash S[1]
[1]Electrical and Electronics Engineering, Bharath Institute of Higher Education and Research, Tambaram, Chennai, Tamilnadu, India.
gbjosly2012@gmail.com

Abstract. The integration of renewable energy sources for Electric Vehicle (EV) charging presents significant challenges, including energy intermittency, voltage fluctuations, and the need for efficient power management. Current electric vehicle (EV) charging systems often face challenges in maximizing charging efficiency, optimizing battery health, and reducing grid dependency, particularly in conditions with variable renewable energy sources. To address these challenges, this paper proposes an intelligent renewable energy-powered onboard EV charger that integrates an Adaptive Neuro-Fuzzy Inference System (ANFIS) and a PID controller tuned by using the self-adaptive Snake Optimization Algorithm (SA-SOA). The Snake Optimization algorithm is utilized to optimize the parameters of both the ANFIS- PID controllers, enabling the system to achieve superior performance by minimizing charging time, reducing energy losses, and improving system efficiency. The system uses a Quasi-Z Source Converter (QZSC) to maintain stable voltage regulation, ensuring optimal charging even with fluctuating input power from renewable sources. ANFIS is employed to dynamically adjust the charging parameters, allowing for adaptive decision-making. The PID controller ensures precise regulation of the charging process, improving system stability and responsiveness. The MATLAB/Simulink simulation platform is used to model and evaluate the performance of the proposed system, demonstrating its capability to optimize energy flow, stabilize voltage, and enhance charging efficiency under various conditions. The primary objective of this work is to develop a smart and energy-efficient onboard charger that maximizes the use of renewable energy, minimizes grid dependency, and ensures optimal charging conditions for EV batteries.

Keywords: EV, ANFIS-PID controller, Self-Adaptive Snake Optimization algorithm, QZSC.

1 Introduction

An EV, or electric vehicle, is a car that operates on rechargeable batteries, offering an environmentally friendly alternative to traditional fuels [1]. EV uses an onboard charger

S. P. Vijayaragavan et al. (eds.), *Proceedings of the Global Conference on Sustainable Energy Systems, Smart Electronics and Intelligent Computing (GCSESEIC 2025)*, Advances in Engineering Research 297,
https://doi.org/10.2991/978-94-6239-654-8_20

(OBC) to charge the batteries, converting AC power from the grid or renewable resources into DC voltage. OBC also facilitates bidirectional energy transfer for V2G, or vehicle-to-grid applications [2]. Onboard battery OBC chargers are crucial. for safe, efficient, and controlled battery charging, protecting batteries from overcharging and optimizing useful life [3]. They can connect renewable resources, maintain grid stability, and offer increased charging flexibility, making OBCs crucial for sustainable transportation and lowering dependency on cars that run on fossil fuels [4].

Onboard chargers in EVs are flexible and convenient, but have significant drawbacks. They impact vehicle efficiency due to their weight and space, limit charging speed, and require specific control strategies [5]. Dual Active Bridge (DAB) converter designs increase cost and complexity, while V2G-enabled boost converter systems suffer from variable switching frequency and higher acoustic noise [6]. Multiport premium vehicles, grid, and PV integrated onboard chargers also have higher system costs, operational complexity, and require multiple converters for precise component selection [7]. Z-source inverter topologies for multiport operation also have limitations [8].

EVs utilize onboard chargers with different converter topologies and control strategies for efficient grid-to-vehicle and vehicle-to-grid activities. fuzzy logic-controlled DC-DC bidirectional converter is sometimes used for optimizing vehicle performance and power management [9]. Some designers use Active neutral point clamp (ANPC) topology in both directions for efficient DC-DC conversion, while others use coupled-inductor power PFC, or factor correction topologies and closed-loop DC-DC stages to reduce losses and overshoot [10]. Onboard chargers also use Z-source counterpart DC-DC boost converter with switching capacitors (SCZEBC) topology, which is fuzzy logic controlled, for solar and fuel cell microgrid charging integration.
The rise in EV usage necessitates sustainable and efficient charging solutions, especially with the adoption of renewable energy sources]. The process presents logistical challenges such as intermittent energy, voltage fluctuations, and precise power management . Current charging solutions often result in reduced efficiency and battery health issues, leaving us reliant on the electrical grid . This study aims to provide an intelligent onboard charging system focusing on renewable energy, integrating an ANFIS with standard PID control and Snake Optimization to avoid energy loss, limit charging time, and offer green EV charging with minimal grid reliance.

The main contribution of this document is as follows,

- The Intelligent ANFIS-PID Control Strategy combines ANFIS and PID for intelligent, accurate EV charging, ensuring efficient and sustainable use of renewable energy.
- The Self-Adaptive Snake Optimization Algorithm (SA-SOA) optimizes ANFIS and PID parameters, increasing charging efficiency, reducing energy losses, and optimizing charging process timing.

- The design incorporates a Quasi-Z Source Converter for stable voltage regulation and optimal energy conversion, ensuring reliable and effective EV charging, even with fluctuating sustainable energy sources.

The way this paper is organized discusses the integration of EVs with renewable energy sources and the requirement for effective onboard chargers in Section 1. It reviews various EV charging technologies and control strategies, highlighting the need to consider renewable energy variability in Section 2. The proposed methodology, ANFIS-PID charging strategy, is designed and combined with the Self-Adaptive Snake Optimization Algorithm and QZSC for voltage regulation in Section 3. The MATLAB/Simulink simulation results demonstrate superior efficiency, charging time, and voltage stability in Section 4. The paper is concluded in Section 5. and the future scope of the paper.

2 Literature Survey

In 2023, Pescetto et.al., examined that the quick uptake of EVs is motivating a need to smaller and more integrated e-axle architectures. This paper proposes a battery charger on board integrated utilizing the traction drive for road EVs using a traction motor drive with six phases. The charger aims to provide a small, low-cost e-axle solution while maintaining galvanic isolation, a unique feature among fully integrated chargers. The The e-drive powertrain has a deeply integrated charger., allowing for the use of any new power device for a traction drive. Dedicated control solutions are developed, demonstrating the use of grid current in AC regulation at unity power ratio with low THD. The charge control must avoid torque production or rotor movement as a secondary effect [1].

In 2024, Hadji et.al., presented An EV's On-board battery charger that is bidirectional consisting of a DC that is bidirectional-DC converter and an AC-DC converter in both directions. What first component uses a P-SVM-DPC modulation technique, while the second uses a direct current control strategy to control battery power and current flow orientation. What selection of these components considers grid-to-vehicle (G2V) and power transfer from vehicles to the grid (V2G) paths. The converter between DC and DC functions as a boost converter or buck converter based on the charge or discharge stage [2].

In 2025, Munusamy & Vairavasundaram examined the efficiency of a three-phase bidirectional converter based on the Adaptive Neuro-Fuzzy Inference System (ANFIS) for Vehicle-to-Grid (V2G) services. controllers and controllers that are proportional-integral (PI). Controllers for ANFIS are unique as they can learn and adapt to different circumstances, providing better real-time control, accuracy, and flexibility. The primary goals include regulating the voltage of the DC connection, reduce THD, or overall harmonic distortion, as well as reduce errors. The transformation of SRF, or the

Synchronous Reference Frame transforms three-stage air conditioning to a two-axis apparatus [3].

In 2024, Bharti et.al. explored the potential of EVs to improve stability of the power grid by utilizing their capacity to store energy for supplementary services like Voltage control and rotating reserves. With high energy consumption and climate change being global issues, EVs could alleviate some of the problems caused by fossil fuel energy consumption. The paper discusses the challenges of integrating a large number EVs into the country's grid, creating better profiles of loads, smarter Both supply and demand management, and lower costs associated with producing energy. It also discusses the scale and impact of EV integration on the power grid, focusing on aspects such as charging times, station availability, state-of-charge estimation, and charging methods [4].

3 Proposed Methodology

The proposed methodology aims to create an intelligent renewable energy-based onboard charger for electric vehicles (EVs), addressing issues like intermittency, voltage variation, and maximum charge efficiency. The working principle is based on PID-equipped System of Adaptive Neuro-Fuzzy Inference (ANFIS) controllers and a Self-Flexible Snake Optimization Algorithm (SA-SOA) embedded within a QZSC stands for Quasi-Z Source Converter. The goal is to maximize renewable energy utilization, stabilize varying inputs, regulate voltage, reduce charge time and efficiency, and preserve battery life by facilitating a controlled and stable charging profile. The components include (RES), (QZSC), (ANFIS–PID hybrid control), (SA-SOA), and (EV battery management). The methodology captures renewable energy flow and adaptive controls for smooth transition, delivering a stable, optimized, and efficient charging profile with reduced reliance on the utility grid. The methodology will develop system functionality and utility, fine-tuning variable parameters for optimal performance, and ensuring site sustainability. Fig. 1 displays the block diagram of proposed.

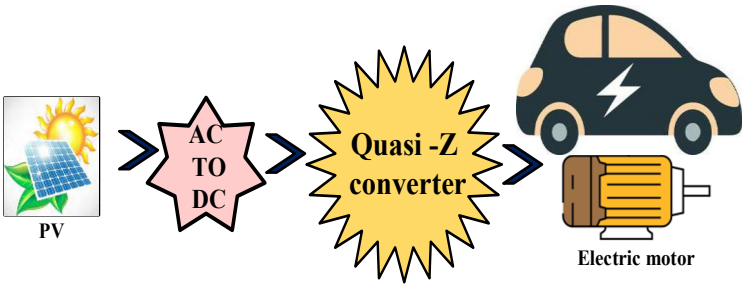

Fig. 1. Block Diagram

3.1 System Architecture

The three principles for the proposed renewable energy-based multifunctional onboard charger for EVs include Renewable Energy Source (RES) Integration, Quasi-Z Source Converter (QZSC), and Intelligent Control Unit optimized by the SA-SOA technique using ANFIS-PID. By integrating those principles, it is capable of maintaining an efficient and comprehensive charging performance under unstable renewable conditions Fig. 2.

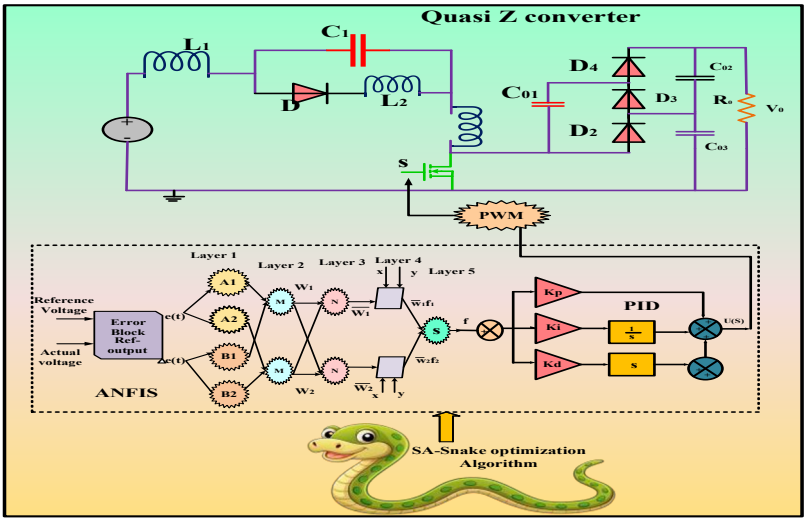

Fig. 2. Architecture for proposed methodology

3.2 ANFIS-PID Hybrid Control Strategy

The proposed hybrid control approach utilizes ANFIS and a PID controller for robust, efficient charging in dynamic environments with renewable energy inputs. It aims to determine charging algorithm parameters, maintain voltage and current stability, and minimize charging time and error. For a two-input ANFIS (input variable is battery SOC and battery voltage).

Fuzzification: each input is mapped into fuzzy sets with a membership function,

$$\mu_{Ai}(s) = \frac{1}{1+\left(\frac{s-c_i}{a_i}\right)^{2b_i}}, \mu_{Bi}(v_{bat}) = \frac{1}{1+\left(\frac{v_{bat}-d_j}{P_j}\right)^{2q_i}} \quad (1)$$

Where $\boldsymbol{a_i}$,$\boldsymbol{b_i}$,$\boldsymbol{c}$,$\boldsymbol{d_j}$,$\boldsymbol{p_j}$,$\boldsymbol{q_j}$ are adaptive parameters tuned by optimization. If S is $\boldsymbol{A_i}$ and $\boldsymbol{v_{bat}}$ is $\boldsymbol{B_j}$ then,

$$f_{ij}(\tau) = \gamma_{ij}S(\tau) + \delta_{ij}v_{bat}(\tau) + \zeta_{ij} \quad (2)$$

ANFIS output is

$$\mu_{\text{ANFIS}}(\tau) = \frac{\sum_{ij}\left[\mu_{A_i}(S).\mu_{B_j}(v_{bat}).f_{ij}(\tau)\right]}{\sum_{ij}\left[\mu_{A_i}(S).\mu_{B_j}(v_{bat})\right]} \tag{3}$$

This is the output that provides adaptive setpoints for charging voltage and current.

The ANFIS layer learns the nonlinear dynamics of the charging process through fuzzy inference rules combined with neural network-based parameter tuning. The PID Layer refines the ANFIS setpoints by correcting deviations between the reference signals $\boldsymbol{v_{ref}(\tau)}$ and the actual charger output $\boldsymbol{v_{out}(\tau)}$

.

In hybrid integration, the final control signal applied to the charger is,

$$u_{\text{hybrid}}(\tau) = \alpha u_{\text{ANFIS}}(\tau) + (1-\alpha)u_{\text{PID}}(\tau) \tag{4}$$

Where $\boldsymbol{\alpha \in [0,1]}$ is a dynamic weighting coefficient determined by system operating conditions.

The hybrid integration of a charger involves a final control signal, which is influenced by a dynamic weighting coefficient. The ANFIS variable control reference regulates the charging process accurately, while the PID variable control reference optimizes the system for the lowest power consumption layer. This system offers adaptive energy utilization, default error minimization, and operational stability irrespective of charging variations

3.3 Snake Optimization Algorithm

One metaheuristic is the Snake Optimization Algorithm (SOA). designed to mimic the social and survival behaviors of snakes, such as mating, fighting, hunting, and nesting, by mathematically modeling their behaviors to balance exploration and exploitation, based on temperature and food availability.

Initialization: N candidates in the population snakes is randomly distributed in the search space,

$$S_i = S_{\min} + \text{rand} \times (S_{\max} - S_{\min}) \tag{5}$$

Where $\boldsymbol{S_i}$is the position of the ith snake, and $\boldsymbol{S_{min}}$, $\boldsymbol{S_{max}}$ are the lower and upper boundaries of variables.

Population Division: The population of snakes is divided separate groups for men and women.

$$N_m = \frac{N}{2}, N_f = N - N_m \tag{6}$$

Where $\boldsymbol{N_m}$ and $\boldsymbol{N_f}$ are the proportions of men and women. Environmental conditions: The algorithm incorporates environmental effects,

$$\text{Temperature decay,} \qquad \text{Temp} = \exp\left(-\frac{t}{T}\right) \tag{7}$$

$$\text{Food availability,} \qquad Q = c_1 \times \exp\left(-\frac{t}{T}\right) \tag{8}$$

The Self-Adaptive Snake Optimization Algorithm (SA-SOA) enhances the original Snake Optimizer's performance by introducing a self-adaptive factor η(t) that adjusts the algorithm's exploration and exploitation behavior according to the iteration number, thereby achieving a better balance between diversity and convergence.

Proposed Self-Adaptive Version

$$\boldsymbol{S_{i,m}(t+1) = S_{\text{rand},m}(t) \pm \eta(t) \cdot c_2 \cdot A_m \cdot (S_{\min} + \text{rand} \cdot (S_{\max} - S_{\min}(S)\mathbf{A} - \mathbf{1})} \tag{9}$$

Where $\boldsymbol{\eta(t) = 1 - \frac{t}{T}}$: A linearly decreasing self-adaptive factor. At $\boldsymbol{t = 0, \eta(0) = 1}$: full exploration. At $\boldsymbol{t = T, \eta(T) = 0}$: full convergence. $\boldsymbol{t}$: current iteration. $\boldsymbol{T}$: maximum iteration. The adaptive modification of the algorithm involves dynamic search adjustments, avoiding premature local optimization, and preserving diversity in early iterations. The randomization factor η(t) reduces snake movement step size, allowing global search and free exploration in the first iterations. The linear learning rate enhances the algorithm without adding additional hyperparameters or creating contention. Fig. 3, 4 illustrate the fighting Mode and Mate Mode

Fig. 3. Fighting Mode

Fig. 4. Mate Mode

Exploitation Phase (food availability)

If Q≥0.25, snakes either hund food or interact(fight/mate) depending on temperature

Hot condition (Temp>0.6): snakes move towards food,

$$S_{i,j}(t+1) = S_{food}(t) \pm c_3 \times \text{Temp} \times \text{rand} \times (S_{food} - S_{i,j}(t)) \tag{10}$$

Cold conditions (Temp≤0.6): snakes fight or mate,

Fighting behaviour (male)

$$S_{i,m}(t+1) = S_{i,m}(t) \pm c_3 \times F_M \times \text{rand} \times \left(Q \times S_{best,f} - S_{i,m}(t)\right) \quad (11)$$

Egg Laying and Population Update

Worst-performing individuals are replaced by new random solutions:

$$S_{morat} = S_{min} + \text{rand} \times (S_{max} - S_{min}) \quad (12)$$

SO provides a biologically similar framework for optimization problems, used in renewable energy systems, EV charging, scheduling, and engineering design, allowing exploration, environmental adaptation, and environmental adaptation.
The ANFIS-PID control scheme is a novel approach to optimizing the tuning of parameters for the PID coordinator, overcoming the limitations of conventional tuning strategies. The study attempts to show the effectiveness of the SA-SOA in parameter optimization, demonstrating its robustness under transient behaviors and faster convergence than static SO and traditional metaheuristics. The SA-SOA algorithm is described in five steps: initialization, self-adaptive exploration/exploitation, fitness evaluation, population update, and convergence.

$$J = w_1 \times ITAE + w_2 \times E_{loss} + w_3 \times T_{ch} \quad (13)$$

Where ITAE: Integral of Time-weighted Absolute Error, E_{loss}: total charging energy loss, $\boldsymbol{T_{ch}}$: charging time. $\boldsymbol{w_1, w_2, w_3}$: weighting factors representing operational priorities.

The SA-SOA algorithm generates initial candidate solutions for membership parameters, adapts its search intensity with each iteration, evaluates fitness using the cost function, updates populations, and keeps on till the minimum error index is attained or the greatest quantity of iterations is achieved. The main advantages of using SA-SOA are its adaptability in learning, multi-objective optimization, and suitability for applications. It prevents premature convergence and works simultaneously on efficiency, charging speed, and stability performance while maintaining robustness under solar and wind renewable fluctuations. This makes SA-SOA an appropriate method for intelligent onboard charging systems of electric vehicles.

4 Results and Discussions

The study demonstrates that the proposed control and optimization strategies enhance system stability, accuracy, and efficiency. The system showed fewer overshoots, reduced settling times, lower RMSE, and better steady-state performance compared to existing methods. It also managed energy flow more effectively in dynamic operating

conditions, rejected disturbances more efficiently, and maintained high output power quality. The design is not only effective but also scalable for practical application.

4.1 Performance Evaluation

The proposed control and optimization strategies outperformed existing methods in various scenarios, resulting in reduced overshoot, reduced RMSE, shorter settling times, and improved accuracy in steady-state. They also enhanced system response in voltage regulation and energy flow situations by reducing oscillation and stabilizing the system faster. The tracking errors and peak deviations were consistently smaller in optimal charging situations, enhancing system robustness against fluctuating, dynamic displacement inputs. Efficiency values were higher in all scenarios, reaching up to 95%, and harmonic distortion was minimal, resulting in better power quality. The upgrades enhanced system accuracy and stability, ensuring energy-efficient and reliable performance.

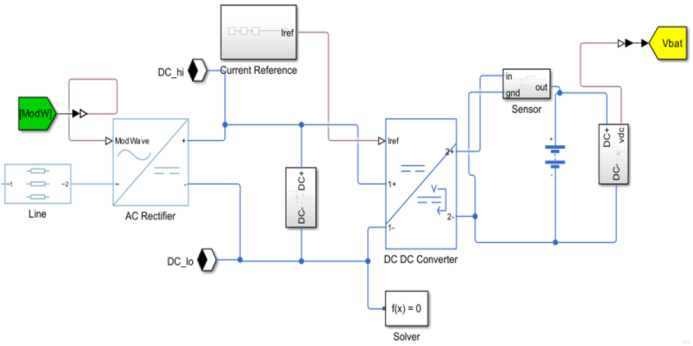

Fig. 5. Block Diagram of AC–DC and DC–DC Power Conversion System

Fig. 5 illustrates a power conversion technology that combines Stages of AC to DC and DC-DC conversion for efficient energy use. The first stage involves an AC line input, which passes through an AC rectifier to produce a regulated DC output. A current reference block ensures stable operation. The converter between DC and DC uses the regulated DC output, providing voltage as well as current to match load needs. A constant current sensor provides input about output conditions, and feedback is required to determine if the output is appropriate for meeting the load and ensuring stability. The final block is the power solver block, which calculates the current value to ensure proper operation, taking into account dynamic constraints. The system then delivers power to the battery, Vbat.

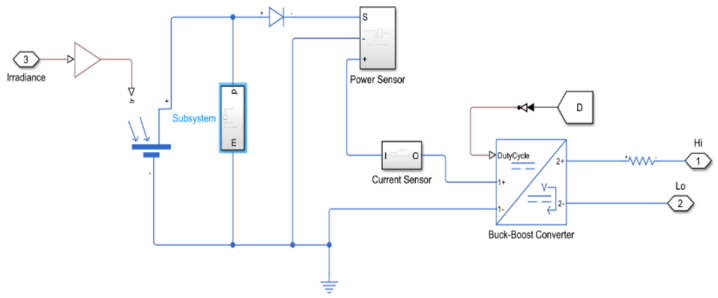

Fig. 6. Block Diagram of PV System Buck-Boost Converter and Sensors

Fig.6 illustrates the photovoltaic (PV) energy conversion system, which involves irradiance control for generating electrical energy. A subsystem manages the output of the PV section, using a diode to prevent reverse current flow. The generated energy input is monitored by power and current sensors, providing performance information via feedback signals. The buck-boost controller regulates the input/output voltage in relation to the duty cycle signal, allowing the converter to increase or decrease in accordance with load input requirements. Factors that could fluctuate between the generated energy input and the regulated output, considering environmental input, differ. The output regulated by the buck-boost converter supplies energy to the connected load, ensuring efficient utilization of generated energy into the plug load connected.

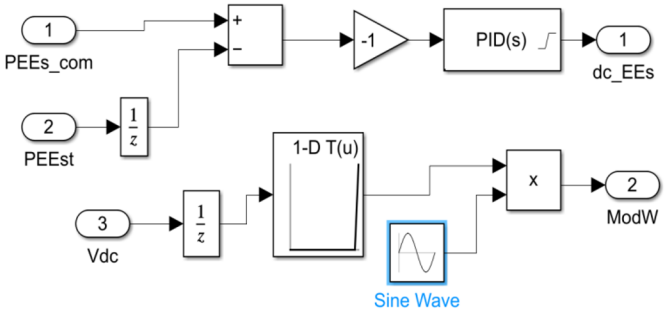

Fig. 7. Control Scheme for Energy Estimation and Modulation Using a PID Controller

Fig. 7 demonstrates the PID-based control scheme for power electronic energy estimation and modulation, which involves comparing a reference command signal to the estimated energy. The error is amplified by a gain, creating a control signal for dc_EEs. A delay in DC voltage, Vdc, is sent to a sine wave generator, forming Modulation (ModW). The modulation waveform is multiplied by the reference output to ensure proper synchronization and regulation of switching signals. This structure

provides energy estimation, minimizes error, and ensures the performance and stability of the power conversion system control

PID controllers consistently outperformed the PI in voltage regulation, settling time 0.6 s vs 1.2 s, overshoot 6% VS 12%, and steady state error 0.01 vs 0.05. PID controllers had more end tracking error and RMSE in optimal charging and variable input power. For energy flow control, PID controllers had better settling time and overshoot, minimizing voltage variance, and achieved better efficiency. The PID controller also minimized the voltage variance, and achieved better efficiency 95% vs, 88%, confirming greater robustness and accuracy for PID controller performance.

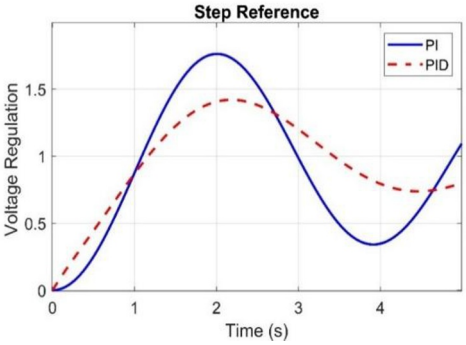

Fig. 8. Voltage Regulation Step Response of PI and PID Controllers

Fig. 8 shows that a PI controller has a significant overshoot and peak voltage regulation of 1.8V, taking time to reach a steady state again. Conversely, the controller for PID has a more stable response with a peak of 1.4V at 2.1 seconds. It settles faster and has less oscillation, improving system stability and reducing overshoot. The derivative term helps decrease system oscillation, reducing overshoot. The final steady-state value for both controllers is around 0.8V. The PID controller provides the most optimal transient response less overshoot and quicker settling time.

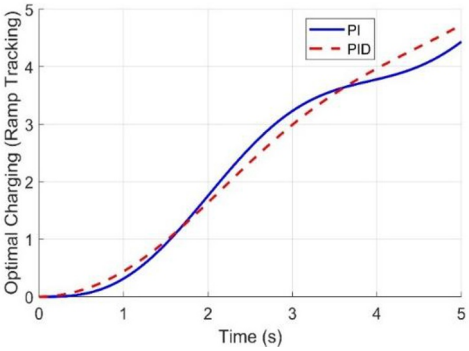

Fig. 9. Optimal Charging Response of PI and PID Controllers

Fig. 9 demonstrates that the PI controller and the PID controller both have a similar tracked response, initially ramping the ramp signal. The PID controller has a more accurate and faster ramping response, indicating that it must always be closer to the ideal ramp than the PI controller to avoid disturbances in the error. At time = 4 seconds, the PID is approximately 4.0V, while the PI is just below that. At time = 5 seconds, the PID response is 5.0V, while the PI response is 4.5V. The PID controller's superior performance is due to the derivative part, which smooths out ramping and reduces lag in obtaining step input points or values. Its design window has no bounds, as applications are often dynamic, while PI controllers are static.

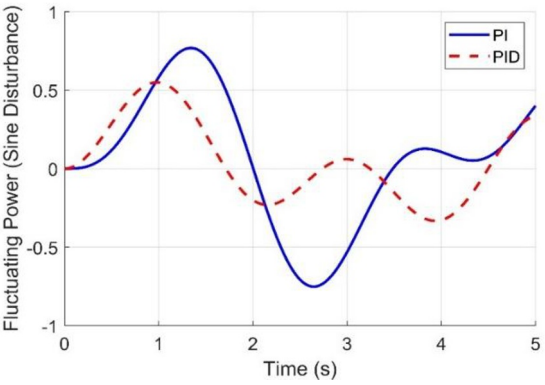

Fig. 10. Fluctuating Power Response to Sine Disturbance

Fig. 10 demonstrates that the PI controller has large output fluctuations, a maximum positive value of +0.8V and a maximum negative value of -0.7V, indicating difficulties in dampening sinusoidal disturbance and large oscillations. Conversely, the PID controller has superior disturbance rejection, less output fluctuations, and faster output return to steady state. The derivative term better predicts and counteracts disturbance, resulting in a more stable system output. The controller of PI's output returns to a stable condition faster, and the oscillations are smaller, indicating its superior performance.

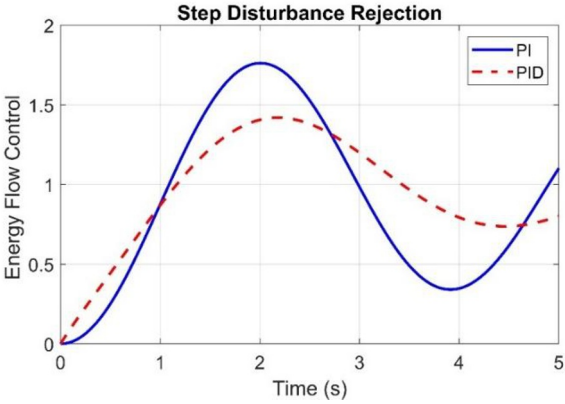

Fig. 11. Energy Flow Control under Step Disturbance

Fig. 11 shows that a PI controller exhibits oscillation in energy flow, reaching a top value of 1.8V at 2.1 seconds and undershooting. It shows little damping and slow stabilization. The PID controller, on the other hand, shows better performance, good stabilization, lower top value, quicker settling, and less oscillation. Its superior performance is due to its aggressive reaction to the derivative term, reducing transient response and allowing it to reject disturbances more quickly, indicating its superior performance under sudden disturbances. Table 3 shows the **Performance** Comparing Intelligent Control Strategies

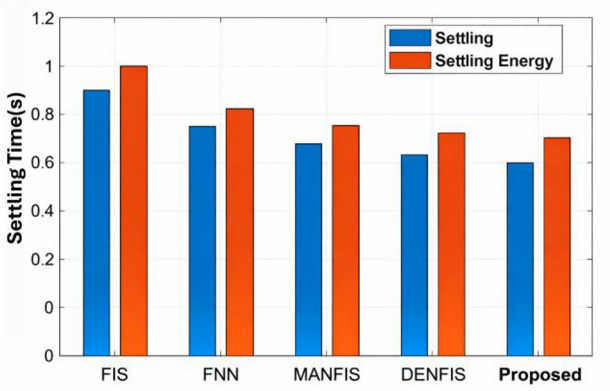

Fig. 12. Comparison of Settling Time and Settling Energy for Various Controllers

Fig. 12 compares the performance of various control systems, focusing on settling time and settling energy. The controllers compared are the Fuzzy Neural Network (FNN), Fuzzy Inference System (FIS), the Modified Adaptive Neuro-Fuzzy Inference System (MANFIS), The Changing and Dynamic Neuro-DENFIS, the Fuzzy Inference System and the proposed controller. The figure shows that the FIS controller has the longest settling time, 0.9s, and the shortest settling energy of 1.0J. The proposed

controller, which System of Adaptive Neuro-Fuzzy Inference, achieved a settling time of 0.6s and the cheapest settling energy of 0.7J. The middle controllers were FNN 0.7s and settling energy of 0.8J, MANFIS 0.65s and settling energy of 0.75J, and DENFIS 0.62s and settling energy of 0.72J. The data indicate that the proposed controller is the most successful in optimizing both metrics and achieving faster and more efficient responses.

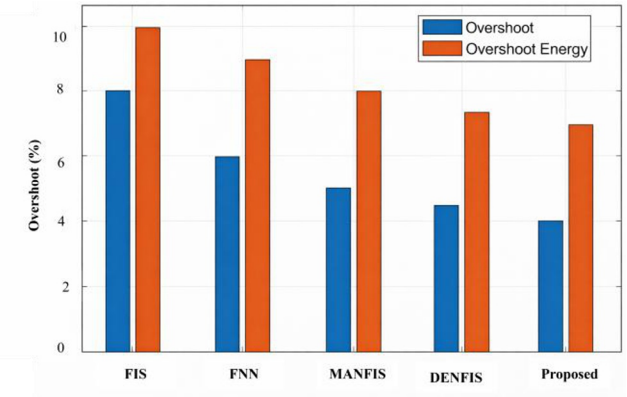

Fig. 13. Overshoot and Overshoot Energy Comparison of Various Controllers

Fig. 13 shows that, comparing control system performance metrics, overshoot percentage, and energy were compared. The Proposed controller showed the best performance, with the lowest values for both metrics. The FIS controller was the worst performer, with an overshoot of 8.0% and an energy of 10.0%. The FNN and MANFIS controllers fell between the controls, but still not as good as the DENFIS controller. The proposed controller was most successful in reducing transient oscillations and energy loss, resulting in a more stable and reliable system response. The data suggests that the proposed controller is the most successful in achieving this goal.

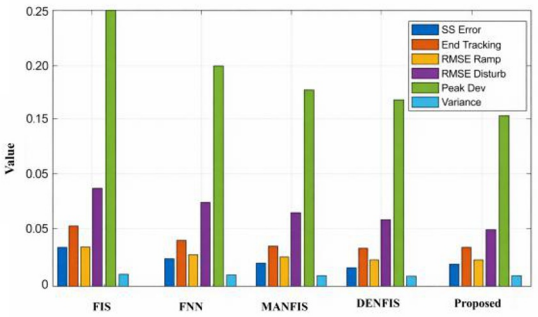

Fig. 14. Performance Metrics of Different Control Systems

Fig. 14 compares five controllers based on metrics such as Steady-State Error, End Tracking, RMSE Ramp, RMSE Disturb, Peak Deviation, and Variance. The

Proposed controller outperforms the other controllers in all but two metrics. The proposed controller possessed the lowest RMSE. Disturb of 0.05, the lowest End Tracking of 0.03, and the lowest Variance of 0.01. Conversely, the FIS controller performed the worst overall the highest Peak Deviation at 0.25, and the highest RMSE Disturbance ≈ 0.09. The proposed controller is able to reduce the error metrics, and it would be able to provide a more accurate and stable control response. Table 1 shows the Comparison of Optimization Algorithms' Performance

Table 1. Performance Comparison of Optimization Algorithms

Optimization	Overshoot (%)	RMSE	efficiency	THD (%)
SSA	6	0.06	92	2.8
ABC	6.5	0.065	91	2.5
PSO	7	0.07	90	1.85
GWO	6.8	0.068	91	1.5
Proposed	5	0.05	95	1.02

Table 1 compares the performance of different optimization techniques, Salp Swarm Grey wolf optimization (GWO), algorithm, artificial bee colony (ABC), and particle swarm optimization (PSO) (SSA), and the proposed method, based on overshoot, RMSE, efficiency, and THD. SSA has a 6% overshoot, a 92% efficiency, and a 2.8% THD. ABC has a 6.5% overshoot, a 91% efficiency, and a 2.5% THD. PSO has a 7% overshoot, a 90% efficiency, and a 1.85% THD. GWO has a 6.8% overshoot, a 91% efficiency, and a 1.5% THD. The proposed method is the best, with the lowest overshoot, RMSE, highest efficiency, and lowest THD.

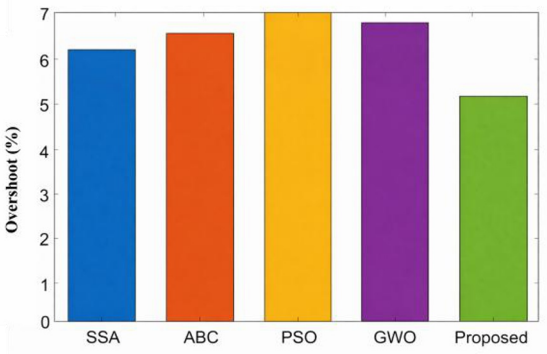

Fig. 15. Overshoot Percentage of Different Optimization Algorithms

Fig. 15 demonstrates the performance of various optimization algorithms, including Spotted Hyena Optimizer (SSA), Grey Wolf, Artificial Bee Colony (ABC), Particle Swarm Optimization (PSO), Optimizer (GWO), and the proposed formula. What Proposed algorithm has the lowest overshoot percentage at about 5.0%, indicating a smaller or less transient oscillatory response. Other algorithms have higher overshoot values, such as SSA at 6.0%, ABC at 6.5%, PSO, and GWO at close to 7.0%. The

Proposed algorithm offers a more stable and efficient system response, making it a better choice over the other benchmarked algorithms.

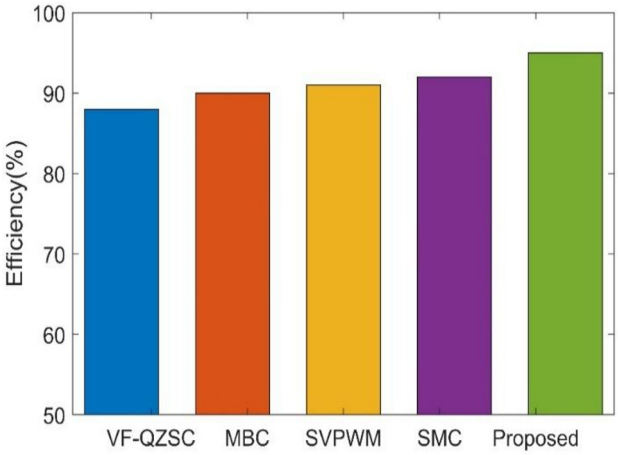

Fig. 16. Efficiency Comparison of Various Control Techniques

Fig. 16 shows that five control techniques were compared, with the Proposed technique showing the highest efficiency at around 95%. This indicates that the control technique minimizes energy loss and maximizes performance. The VF-QZSC technique had the lowest efficiency at 88%. The other three techniques were between the two: the MBC at 90%, the SVPWM at 91%, and the SMC at 92%. The Proposed technique was found to be the most effective and provide the highest level of efficiency, making it the most suitable for the control system.

5 Discussion

The proposed control and optimization strategies outperform common methods like PI, PID, and other intelligent control strategies. The combination of ANFIS-based control and advanced optimization strategies enhances system stability, dynamic performance, efficiency, and power quality. The PID model gains minimal overshoot and settling time, while the ANFIS model provides minimal steady state error, variance errors, and peak deviation. The proposed algorithms outperform SSA, ABC, PSO methods, and GWO mechanisms in terms of overshoot, RMSE, and THD, minimizing and enhancing efficiency. The QZSC approach offers the lowest overshoot, highest efficiency, and lowest RMSE, making it suitable for energy-sensitive applications requiring high precision.

5. Conclusion

The study presents an intelligent renewable energy-based onboard EV charger using ANFIS-PID hybrid control and a self-adaptive Snake Optimization Algorithm with a Quasi-Z Source Converter. The system addresses charging efficiency, voltage stability, and grid dependency issues. Simulation results show it outperforms other intelligent controllers, achieving efficiency. The introduction of SA-SOA optimization offers robust parameter tuning, while the QZSC regulates voltage at variable renewable power inputs. This system has potential for real-world implementation in future EV charging systems, providing a scalable, energy-efficient, and sustainable solution for maximizing renewable energy use with electric vehicles while preserving battery health and reducing power grid dependency.

References

1. Pescetto, P., Cruz, M.F.T., Stella, F., Pellegrino, G.: Galvanically isolated on-board charger fully integrated with 6-phase traction motor drives. In: IEEE Access, vol. 11, pp. 26059–26069 (2023)
2. Hadji, K., Hartani, K., Chikouche, T.M.: New combined control strategy of on-board bidirectional battery chargers for electric vehicles. In: International Journal of Power Electronics and Drive Systems, vol. 15, pp. 303–311 (2023)
3. Munusamy, N., Vairavasundaram, I.: Enhancing grid stability and V2G integration by optimizing three-phase bidirectional EV chargers using ANFIS and FPGA-based control systems. In: Global Energy Interconnection (2025)
4. Bharti, K.P., Ashfaq, H., Kumar, R., Singh, R.: Designing a bidirectional power flow control mechanism for integrated EVs in PV-based grid systems supporting onboard AC charging. In: Sustainability, vol. 16, p. 8791 (2024)
5. Mehmood, A., Yang, F.: Improvement of power quality of grid-connected EV charging station using grid-component based harmonic mitigation technique. In: Energies, vol. 18, p. 2876 (2025)
6. Elkeiy, M.A., Abdelaziz, Y.N., Hamad, M.S., Abdel-Khalik, A.S., Abdelrahem, M.: Multiport DC–DC converter with differential power processing for fast EV charging stations. In: Sustainability, vol. 15, p. 3026 (2023)
7. Kumar, B.A., Jyothi, B., Rathore, R.S., Singh, A.R., Kumar, B.H., Bajaj, M.: Novel framework for enhancing the power quality of electric vehicle battery charging based on a modified Ferdowsi converter. In: Energy Reports, vol. 10, pp. 2394–2416 (2023)
8. Kim, J.-W., Lee, D., Cho, Y.: Series resonant converter with multiple resonant points using sequential PWM for electric vehicle on-board charger. In: IEEE Access, vol. 11, pp. 37920–37930 (2023)
9. Shahed, M.T., Rashid, A.B.M.H.-U.: Improved topology of isolated bidirectional resonant DC–DC converter based on wide bandgap transistors for electric vehicle onboard chargers. In: International Transactions on Electrical Energy Systems, pp. 1–18 (2023)

10. Elezab, A., Zayed, O., Abuelnaga, A., Narimani, M.: High efficiency LLC resonant converter with wide output range of 200–1000 V for DC-connected EV ultra-fast charging stations. In: IEEE Access, vol. 11, pp. 33037–33048 (2023)